Palaeogeography, Palaeoclimatology, Palaeoecology 577 (2021) 110548

Contents lists available at ScienceDirect

Palaeogeography, Palaeoclimatology, Palaeoecology

journal homepage: www.elsevier.com/locate/palaeo

Invited Research Article

Detrital zircon ages reveal Yangtze provenance since the early Oligocene in the East China Sea Shelf Basin

Jingyu Zhang [a,b,c], Wout Krijgsman [b], Yongchao Lu [a,c,*], Jinshui Liu [d], Xiangquan Li [e], Xuebin Du [e], Wei Wei [f], Hao Lin [a]

[a] School of Earth Resources, China University of Geosciences, Wuhan 430074, China
[b] Paleomagnetic Laboratory Fort Hoofddijk, Department of Earth Sciences, Utrecht University, Budapestlaan 17, 3584 CD Utrecht, the Netherlands
[c] Key Laboratory of Tectonics and Petroleum Resources of Ministry of Education, China University of Geosciences (Wuhan), Wuhan 430074, China
[d] CNOOC Shanghai Branch, Shanghai 200030, China
[e] College of Marine Science and Technology, China University of Geosciences (Wuhan), Wuhan 430074, China
[f] School of Earth Sciences, China University of Geosciences, Wuhan 430074, China

ARTICLE INFO

Editor: Paul Hesse

Keywords:
Provenance study
Depositional sink
Eastern Asia
Tibetan Plateau

ABSTRACT

The origin and evolution of the Yangtze River drainage system play a crucial role in the palaeogeographic and palaeoenvironmental evolution of East Asia. The source-to-sink history of this major Chinese river provides information on the initiation of a topographic gradient in East Asia driven by far-field and near-field effects of plate tectonics and elucidates the subsidence and depositional history of the depocenter in the East China Sea Shelf Basin (ECSSB). Unraveling age constraints on Yangtze provenance, however, remains a big challenge. Here, we review U—Pb ages of detrital zircon grains from the Oligocene-Miocene successions of the north ECSSB and perform several statistical tests to quantify mixing proportions of different potential source areas that reveal similar age patterns as the modern Yangtze River. We conclude that the initiation of a modern-type Yangtze drainage was established before ~34 Ma, and confirm that in the Oligocene an eastward drainage system was in place from the Yangtze Craton to the ECSSB where huge depositional systems developed on the Chinese continental margin. Monte Carlo models imply that the Oligocene and Miocene sediments of the north ECSSB were mainly supplied by the Yangtze River and the North China Craton - South Korean rivers, and that during the Miocene (< 23 Ma) the Yangtze drainage system extended further southward, reaching the marginal basins of modern Taiwan.

1. Introduction

The continental collision between India and Eurasia played an important role in influencing Asian tectonics, landforms, and drainage systems (Clark et al., 2004; Wang, 2004; Clift et al., 2008b). Responding to the uplift of the Tibetan Plateau and the changing topography and climate of eastern Asia, the Yangtze River evolved as the largest river with a length of ~6300 km and a catchment area of 1.8 million km^2 (Zheng, 2015; Yang et al., 2019). It originates from the Qiangtang Block on the Tibetan Plateau and drains eastwards into the East China Sea Shelf Basin (ECSSB) (Fig. 1). The evolution of the Yangtze River is characterized by multiple river capture events (e.g., the First Bend and the Three Gorges; Yang et al., 2019), marking the development of a regional topographic gradient (e.g., Cenozoic Topographic Reversal, Wang, 2004). Its large drainage system transports an enormous amount of sediment from the India-Asia collision zone to the marginal seas of eastern China (Métivier et al., 1999; Clark et al., 2004), which act as major depositional sinks (Milliman and Farnsworth, 2013).

The development of the Yangtze River has been the focus of several recent studies, but the age of the initiation of the modern Yangtze drainage system remains unclear, with age estimates ranging from Paleogene (45–40 Ma or 36.5–23 Ma) to Quaternary (2.6–1.7 Ma) (e.g., Li et al., 2001; Xiang et al., 2007; Richardson et al., 2010; Wang et al., 2010; Zheng et al., 2013a; Yue et al., 2016; Wang et al., 2018; Fu et al., 2020). Compared to the wavering location of the ancient Yangtze River delta, resulting from a constantly shifting coastline (Ren et al., 2002), the sedimentary successions of the depositional sinks are more stable (Yan et al., 2011; Shao et al., 2016). The ECSSB is therefore one of the

* Corresponding author at: School of Earth Resources, China University of Geosciences, Wuhan 430074, China.
E-mail addresses: W.Krijgsman@uu.nl (W. Krijgsman), Yongchaolu_2@163.com (Y. Lu), xbdu@cug.edu.cn (X. Du).

https://doi.org/10.1016/j.palaeo.2021.110548
Received 11 December 2020; Received in revised form 2 June 2021; Accepted 24 June 2021
Available online 29 June 2021

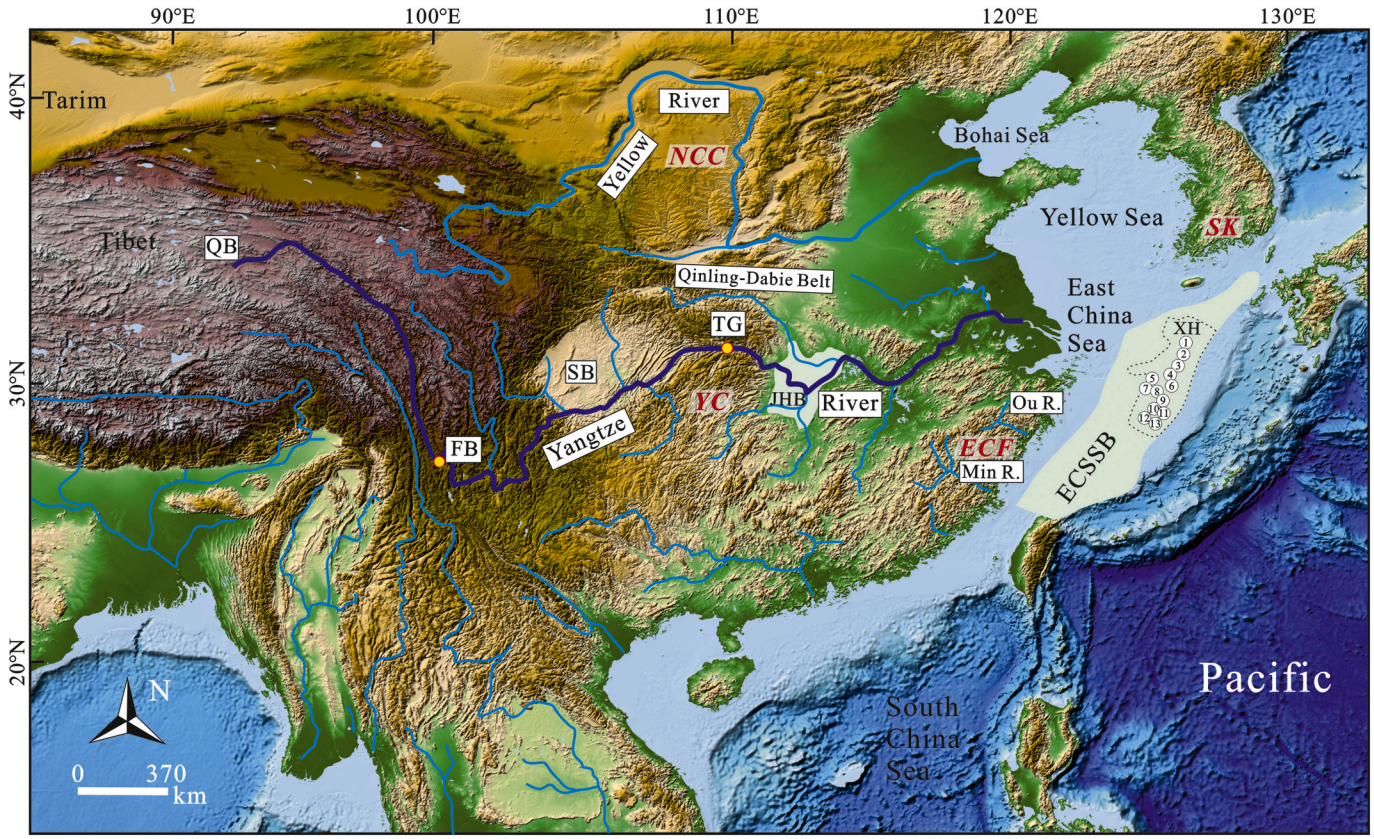

Fig. 1. Geographical map of present-day East Asia. The blue lines are major river systems in East Asia, the dark blue line shows the mainstream of the Yangtze River (modified from Zheng et al., 2013a; Zhang et al., 2017). ECSSB: East China Sea Shelf Basin; XH: Xihu Depression; JHB: Jianghan Basin; TG: Three Gorges; SB: Sichuan Basin; FB: First Bend; QB: Qingtang Block. Numbers 1–13 denote the location of our studied boreholes. Potential sources (red): Yangtze Craton (YC), North China Craton (NCC), South Korea (SK), and East Cathaysia Foldbelt (ECF). The Qinling-Dabie Belt is the boundary between the North China Craton and Yangtze Craton (Zhang et al., 2017). (For interpretation of the references to colour in this figure legend, the reader is referred to the web version of this article.)

best repositories to obtain insights on the evolution of the Yangtze River system. Provenance analysis of its sedimentary record may provide important constraints on the origin and development of the Yangtze drainage diversion.

Recent studies focusing on detrital zircon U—Pb ages from sandstones of the ECSSB resulted in two different hypotheses. Wang et al. (2018) indicate a high degree of similarity between the zircon age spectra of the upper Oligocene Huagang Formation of the ECSSB and the modern Yangtze sediments, suggesting a pre-Miocene initiation of the Yangtze River. Fu et al. (2020), however, observe different age spectra in Cenozoic sediments of the southern and northern ECSSB and subsequently infer that the Yangtze River drainage system was established in the late Miocene. Here, we re-analyse the detrital zircon ages from the Xihu Depression of the ECSSB (Zhang et al., 2018), that includes the Huagang Formation, the underlying lower Oligocene Pinghu Formation, and the overlying lower Miocene Longjing Formation, to verify and better date the Yangtze provenance. We quantitatively determine the potential link between the Yangtze River and the North ECSSB and provide new evidence in the debate on the formation and evolution of the modern Yangtze River drainage system.

2. Geological setting

The ECSSB is located on the eastern margin of the Asian continental plate (Fig. 1), and is one of the major offshore Cenozoic basins in eastern Asia. It is situated at the convergence of the Eurasian Plate, the Pacific Plate, and the Philippine Plate. The Xihu Depression, renowned for its rich hydrocarbon resources, developed during the late Cretaceous to middle Eocene in the northeastern part of the ECSSB (Yang et al., 2010). Its total Paleogene to Quaternary sedimentary succession is approximately 10,000 m thick (Su et al., 2020) and is mainly composed of sandstone and mudstone interbedded with coal seam and limestone (Yang et al., 2010).

The complex tectonic setting of East Asia implies that different source areas could have provided sediments to the ECSSB through multiple drainage systems (e.g., Wang et al., 2018; Fu et al., 2020). In the north, the North China Craton and South Korea form a fundamental part of the Sino-Korean Platform (Huang et al., 1977; Zhao et al., 1993). The North China Craton contains an Archean to Paleoproterozoic metamorphosed basement, which is covered with Mesoproterozoic to Phanerozoic unmetamorphosed rock (Zhai et al., 2005; Zhao et al., 2005; Zhai and Santosh, 2011). South Korean rivers mainly source Cretaceous and Jurassic granite and Precambrian gneiss with minor limestone, schist, volcanic rock, and phyllite (Lee et al., 1988; Chough et al., 2000). The South China Block to the west can be divided into the Yangtze Craton and the Cathaysia Foldbelt (Zheng et al., 2013b). The Yangtze Craton comprises Archean–Paleoproterozoic crystalline basement (Zheng et al., 2006; Zhao and Cawood, 2012), surrounded by late Mesoproterozoic to early Neoproterozoic orogens (Zheng et al., 2013b). The Cathaysia Foldbelt predominantly comprises Neoproterozoic basement rocks with minor occurrences of Paleoproterozoic rock in its eastern part (Yu et al., 2010; Xia et al., 2012; Zhao and Cawood, 2012). The Songpan-Ganzi Terrane and Qiangtang Block, located in the Upper Yangtze River region, are also potential source areas. The Songpan-Ganzi was intruded by Triassic and Cenozoic magmatic rock (Sun et al., 2018), characterized by a folded Triassic flysch complex (Weislogel et al., 2010; He et al., 2013). The Qiangtang Block is mostly covered by Triassic sediments and intruded by Cenozoic magmatic rock

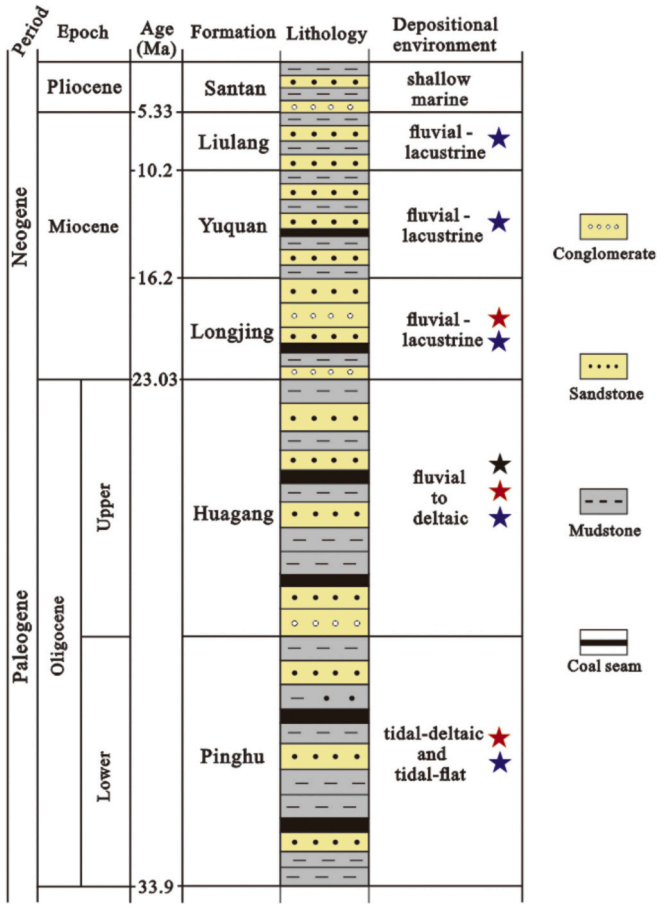

Fig. 2. Simplified lithostratigraphy of the Xihu Depression in the ECSSB where the Oligocene-Miocene deposits are subdivided into Pinghu, Huagang, and Longjing formations (modified from Su et al., 2020). The chronostratigraphy (Abbas et al., 2018) is updated from Zhang et al. (2020), the depositional environments are from Abbas et al. (2018), Li et al. (2018), and Su et al. (2020). Red, black, and blue stars correspond to borehole samples in Zhang et al. (2018), Wang et al. (2018), and Fu et al. (2020), respectively. (For interpretation of the references to colour in this figure legend, the reader is referred to the web version of this article.)

(Van Hoang et al., 2009). The Diaoyu Islands Folded-Uplift Belt to the east mainly comprises Paleozoic metamorphic strata (Yang et al., 2010).

This paper focuses on the Oligocene Pinghu and Huagang, and the Miocene Longjing formations of the Xihu Depression (Fig. 2). The Pinghu Formation mainly consists of sandstone, silty mudstone, and mudstone with coal seam, interpreted as tidal-deltaic and tidal-flat deposits (Zhao et al., 2008; Zhu et al., 2012; Wu, 2016; Abbas et al., 2018; Li et al., 2018). The Pinghu sediments are considered to be the primary hydrocarbon source rock of the Xihu Depression (Zhu et al., 2012). A recent cyclostratigraphic analysis, combined with U—Pb dating, indicated that the sequence stratigraphic framework of the Pinghu Formation is best constrained to the early Oligocene (Zhang et al., 2020). The overlying Huagang Formation comprises an alternation of sandstone and mudstone and is interpreted to have been deposited in fluvial to deltaic environments (Hao et al., 2018a). The Huagang Formation is the main hydrocarbon reservoir in the Xihu Depression and its depositional environment shows a complex provenance pattern with sedimentary transport paths from the west, north, and east (Zhang et al., 2018). The Huagang Fm. is generally attributed to the Oligocene based on biostratigraphic constraints (Ye et al., 2007; Suo et al., 2015). According to Zhang et al. (2020), the Huagang Formation correlates best to the late Oligocene. The Miocene Longjing Formation overlies the Huagang Formation and was deposited in fluvial and lacustrine environments (Zhu et al., 2010; Zhang et al., 2012).

3. Sampling and methods

Eighteen samples were used for detrital zircon U—Pb geochronology analysis from thirteen petroleum exploration wells in the Xihu Depression at 124°27′–127°00′E and 27°30′–30°59′N (Fig. 1), as previously reported by Zhang et al. (2018). Two samples were collected from the Pinghu Formation, thirteen samples from the Huagang Formation, and another three from the Longjing Formation (Fig. 2). Analytical work on U—Pb dating was conducted by Laser Ablation Inductively Coupled Plasma Mass Spectroscopy (LA-ICP-MS) and was done at the State Key Laboratory of Geological Processes and Mineral Resources, China University of Geosciences (Wuhan). Laser Ablation analysis was performed on a GeoLas 2005, and the ICP-MS measurements were done on an Agilent 7500a. Each study included a 20-s gas blank followed by a 50-s data acquisition period. Zircon 91,500 with an age of 1065.4 ± 0.6 Ma (Wiedenbeck et al., 1995), used as an external standard for U—Pb dating, was evaluated twice every six analyses (Ding et al., 2017). The spot diameter was 32 μm at 1σ level of age uncertainties. The ICPMS-Datacal method was used to quantify the U–Th–Pb isotopic ratios (e.g., Liu et al., 2008). The $^{206}Pb/^{238}U$ age is used for young (< 1000 Ma) zircon crystals, whereas older zircon (> 1000 Ma) crystals are expected to have relatively stable $^{207}Pb/^{206}Pb$ ratios (Compston et al., 1992). We only used valid grains with <10% age discordance.

The three-dimensional multidimensional scalar (MDS) in DZmds software of Saylor et al. (2018) was used to study the relationship between the different samples and their putative source areas. The MDS plots usually group the samples with similar age spectra and separate those with different spectra (Cao et al., 2020). In addition, Monte Carlo-based methods for detrital geochronological data were performed to quantify mixing proportions of different potential provenances using DZmix software of Sundell and Saylor (2017). We implemented the cross-correlation coefficient (R2) and K—S test statistic (D) in the modeling to avoid overreliance of any single goodness-of-fit metric. Ten-thousand trials are run to reproduce a particular detrital age spectrum by changing contributions from different sources to match the age spectrum of mixed samples. The results of the mixing analysis are shown graphically in cumulative probability plots.

4. Results

Detrital zircon age distributions are here visualized as kernel density estimates (KDE) by the DensityPlotter program (Vermeesch, 2013), using a 50 Ma adaptive bandwidth (Fig. 3). The detrital zircon U—Pb ages from the Pinghu Formation in the ECSSB yield a wide age range from Archean to early Cenozoic, with two main peaks of 224 Ma and 1845 Ma, and two minor peaks at 793 Ma and 2480 Ma (Fig. 3F). Our results of detrital zircon U—Pb ages from the Huagang Formation show major peaks at 230 Ma and 1844 Ma, and minor peaks at 435 Ma, 773 Ma, and 2485 Ma (Fig. 3E; Zhang et al., 2018). These results are similar to the other age spectra reported from the Huagang Formation that show similar major peaks at 201 Ma and 1850 Ma with minor peaks at 794 Ma, and 2480 Ma (Fig. 3D; Yang et al., 2006; Wang et al., 2018). The age distribution of the zircon grains from the Longjing Formation also shows similar peaks at 225 Ma and 1848 Ma with minor peaks at 441 Ma, 786 Ma, and 2471 Ma (Fig. 3C).

Most sediments in the northeastern ECSSB show five different peaks at ~2470 Ma, ~1850 Ma, ~790 Ma, ~440 Ma, and ~ 220 Ma, similar to the five peaks in the age spectra of the modern Yangtze River (Fig. 3). A key issue here is the relative heights of the ~790 Ma Paleozoic and the two ~2470 and ~ 1850 Ma Precambrium source peaks. We use the same method as Fu et al. (2020) to estimate the proportion of zircons for a more accurate comparison (Table S1). The KDEs of the north ECSSB sediments show a relatively stable contribution of the ~790 Ma component (500 Ma–1000 Ma) in the Pinghu (~10%), Huagang

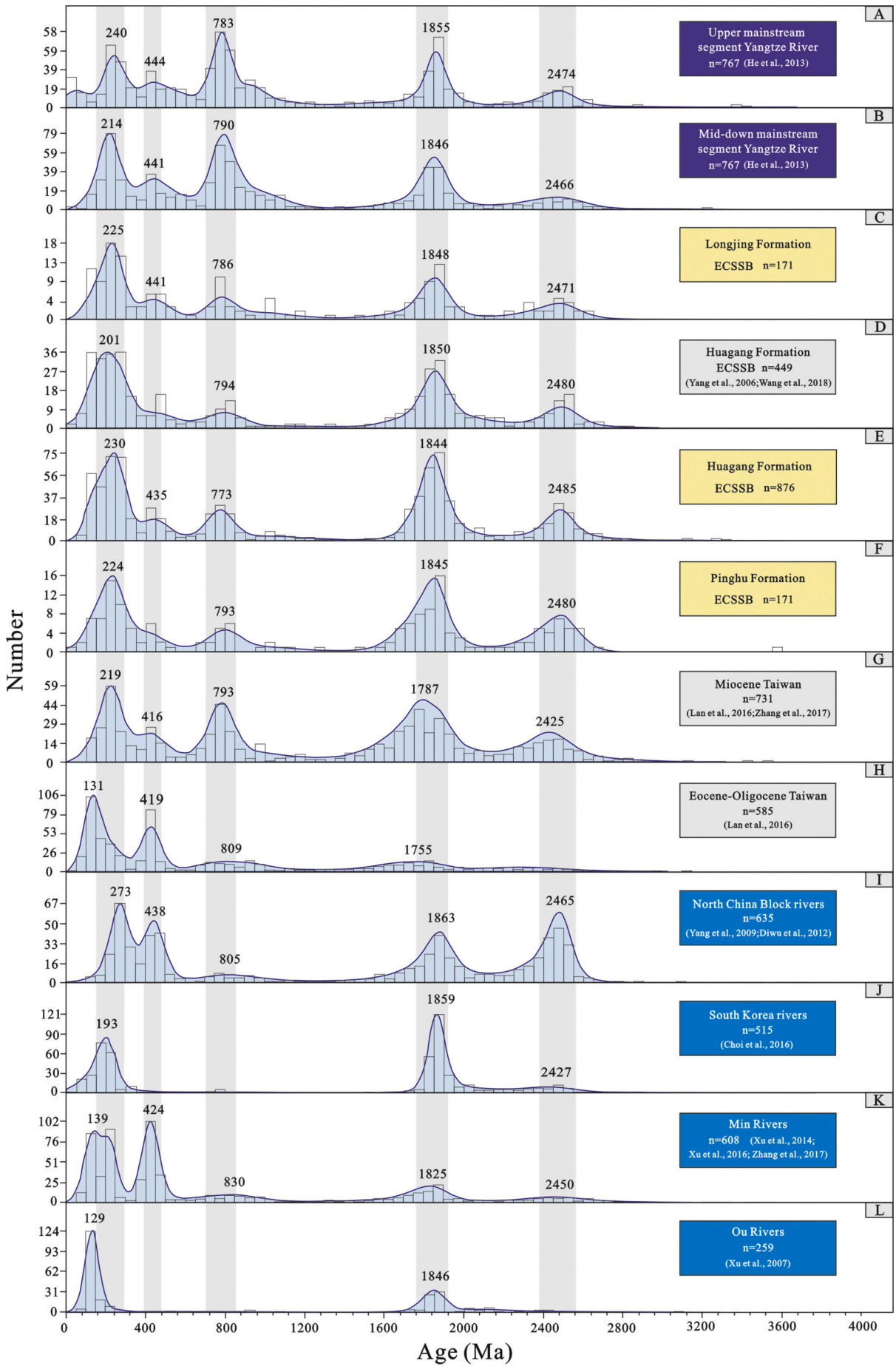

(caption on next page)

Fig. 3. Kernel density estimation (KDE) plots (Vermeesch, 2013) for the zircon U—Pb ages. The dark blue and light blue labels represent data from the Yangtze River and other major SE Asian rivers, respectively. The yellow label denotes the plots with our own data, and the gray label represents data from literature. A and B) modern river sands from the Yangtze River, C) sedimentary strata of the Longjing, D and E) Huagang, and F) Pinghu Formation in the Xihu Depression of the East China Sea Shelf Basin. G and H) represent Eocene to Miocene strata of the Taiwanese margin, respectively. Other major rivers in East Asia: I) North China Craton rivers, J) South Korea rivers, K) Min River, and L) Ou River (see Fig. 1 for their location). (For interpretation of the references to colour in this figure legend, the reader is referred to the web version of this article.)

(~12%), and Longjing (~14%) formations (Fig. 3, Table S1).

In the MDS plots (Fig. 4A), two groups can be identified. The Eocene-Oligocene Taiwan sample links best with the Min River and (roughly) Ou River samples. The Pinghu, Huagang, Longjing, and Miocene Taiwan samples cluster with the Yangtze River, North China Craton rivers, and South Korean rivers samples. The two modeled mixture results are largely similar, with the average contribution of Pinghu, Huagang, and Longjing formations from the Yangtze River provenances showing a range from ~21.9% to ~31.3% to ~45.4% in the R^2-based model and from ~18.7% to ~30% to ~43.4% in the D-based model (Fig. 4B). The mixed results also show an appreciable contribution from the North China Craton rivers (average ~ 38.8% and ~32.6%) and South Korean rivers (average ~ 16.9% and ~20.3%) and a low contribution from the Min River (average ~ 6.9% and ~10.5%) and Ou River (average ~ 4.4% and ~ 5.8%) in the R^2-based and D-based models.

5. Discussion

5.1. The age of the modern Yangtze drainage system

The distribution patterns of detrital zircon U—Pb ages in the Xihu Depression can be compared to the zircon age spectra of other parts of the ECSSB and to the modern river sands of the Yangtze River and the other major East Asian rivers to investigate sediment distribution patterns and the arrival of the Yangtze drainage in the ECSSB. The KDE diagrams from the Pinghu, Huagang, and Longjing formations are all rather similar as indicated by their proximity in the MDS plots, implying stability of the sediment supply during the Oligocene to Miocene in the Xihu Depression (Figs. 3, 4).

In the MDS plots (Fig. 4A), the closest provenance neighbour of the Pinghu, Huagang, and Longjing formations is the Yangtze River, indicating a potential source-to-sink relationship. The KDE of the present-day Yangtze River is, however, characterized by a much higher proportion (20–48%) of the ~790 Ma component (He et al., 2013; He et al., 2014). The Yangtze River is the only East Asian river with a significant proportion of Paleozoic components (Fig. 3). Other major rivers show zero proportions of the ~790 Ma component (South Korean rivers, Ou River; Figs. 3J, L), and/or have much higher additional proportions of the ~420 Ma component (North China Craton rivers, Min River; Fig. 3I, K). The Yangtze is thus the only possible East Asian river drainage explaining the peak at ~790 Ma in the ECSSB. The fact that this peak only contributes to 10–14% of the total age spectrum requires the presence of additional sources with high proportions of ~2470 Ma, ~1850 Ma, and 220 Ma components. Given the overall southward tilt of the ECSSB, this basically excludes provenance from southern sources and these additional components were therefore most likely derived from the north and/or west. The North China Craton and South Korea rivers that drain the northwestern hinterland of the ECSSB are enriched in both Precambrium and Mesozoic components (Figs. 3I, J) and can explain, together with the Yangtze, all the KDE patterns in the Oligocene to Miocene deposits of the Xihu Depression.

Sediment supply in the ECSSB may also have been partly derived from its neighbouring margins. The borderlands in the north comprise Precambrium rocks (e.g. Hupijiao Uplift with Proterozoic metamorphic rocks superimposed on Yanshanian igneous rocks) (Liang et al., 2006; Yang et al., 2010), while Mesozoic components may be derived from the west (e.g. Haijiao Uplift) where Jurassic-middle Cretaceous rocks are available (Yang et al., 2010). The only alternative source of Paleozoic components is the Diaoyu Islands Folded-Uplift Belt to the east of the Xihu Depression, where Paleozoic metamorphic strata form the key bedrock (Yang et al., 2010; Zhang et al., 2018). It is, however, difficult to quantify the relative contribution of these local source regions.

We conclude that the Yangtze River has been an important provenance source for the zircon age spectra of the Oligocene to Miocene sediments in the northern ECSSB. This is in agreement with the interpretation of Wang et al. (2018) who already concluded that the U—Pb age spectra of the Huagang Formation show a high degree of similarity with the spectra of modern sediment from the Yangtze River. Our data show that comparable age spectra were obtained by the older Pinghu Formation (Fig. 3F), indicating that a major Yangtze supply to the ECSSB was already present during the early Oligocene.

5.2. Miocene expansion of the Yangtze drainage system?

Fu et al. (2020) recently concluded, based on age spectra from zircon dating, that the arrival of the Yangtze drainage in the ECSSB was post-early Miocene. They base this on the fact that a dominant peak (25–33%) in the ~790 Ma component (500 Ma–1000 Ma) is only present in the upper Miocene to Pliocene strata of the ECSSB. In their analyses, however, they combined results from two study areas, one in the northern and one in the southwestern part of the ECSSB. It must be noted that a major uplift belt (e.g., Hao et al., 2018b; Feng et al., 2019) is present between these two regions and that Oligocene deposits are lacking in the southwestern part of the ECSSB (Fu et al., 2020).

The contribution of the ~130 Ma component (potential contribution of the Min and Ou Rivers) in the southwestern ECSSB is significantly higher than in the northern basin (Table S1). We speculate that these two regions had different provenance areas and thus represent different branches of the Yangtze drainage. This implies that changes in age spectra must be discussed independently. If we only regard the Fu et al. (2020) results of the northern region (e.g. their N1 well), the age distribution of the ~790 Ma component is rather similar in the Oligocene (~ 8%, ~14%), lower Miocene (~13%), middle Miocene (~15%), and upper Miocene (~22%), and in excellent agreement with our results. Regarding the age spectra of the southwestern region (excluding the anomalous L1 well), the proportion of the ~790 Ma component (J1 and Z1 wells, Table S1) increases from the middle Eocene (14% and 18%) and early Miocene (8% and 17%) to the late Miocene (25%) (Fu et al., 2020).

A change in Yangtze provenance is also suggested from the sedimentary successions of the Taiwan region. The U—Pb age distributions of the ECSSB deposits agree very well with the KDE plots of the Miocene deposits of Taiwan (Fig. 3G) as indicated by their proximity in the MDS plots (Fig. 4A). The Oligocene deposits of Taiwan show significantly different spectra, mainly reflecting the Min River KDE (Fig. 3H; Wang et al., 2018). Some studies (e.g., Lan et al., 2016; Xu, 2017) suggested that these different age spectra are mainly the result of an evolving Min River. However, the increase of ~790 Ma, ~1780 Ma, and ~2420 Ma components is then hard to explain (Fig. 3), and the MDS results indicate that Miocene sediments of the Taiwan region are not dominated by Min River sources.

This similarity between the Miocene Taiwan and Oligocene ECSSB sediments is explained by Wang et al. (2018) through reworking of Huagang or younger successions. These authors also discussed the tectono-sedimentary evolution of the ECSSB and the possibility of a viable dispersal path for sediment towards the Taiwan region. Inversion

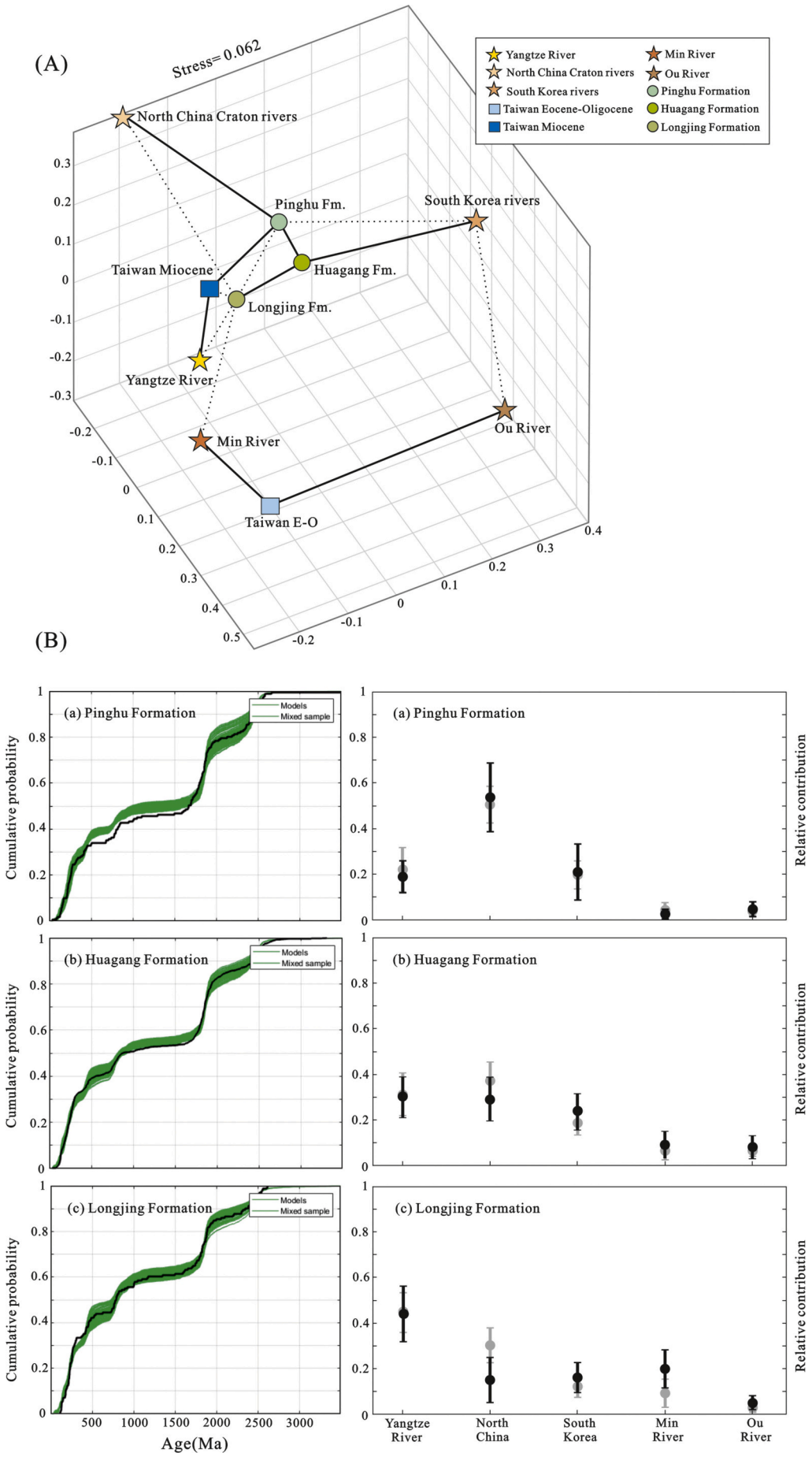

Fig. 4. A) Three-dimension multidimensional scaling (MDS) for detrital zircon ages of target formations and potential provenances. The intersample dissimilarity is calculated as the cross-correlation coefficient of KDE spectra with a bandwidth of 50 Ma. The stress value is 0.062, indicating the desirable goodness-of-fit of MDS statistics. B) Mixture combinations of defined potential provenances for the Pinghu, Huagang, and Longjing formations in the Xihu Depression, generated by the Monte Carlo model (Sundell and Saylor, 2017). Left panel: Cumulative probability plots showing the best fits between the K-S-derived forward models (green) and the observed (black) age spectra in this study. Right panel: Calculated contributions based on the cross-correlation coefficient (R^2) (gray) and the K—S test statistic (D) (black). The mean R^2 and D values are: (a) 0.78 and 0.065, (b) 0.855 and 0.04, (c) 0.843 and 0.055, respectively, generally indicating a high level of confidence. Error bars display 1σ uncertainty. (For interpretation of the references to colour in this figure legend, the reader is referred to the web version of this article.)

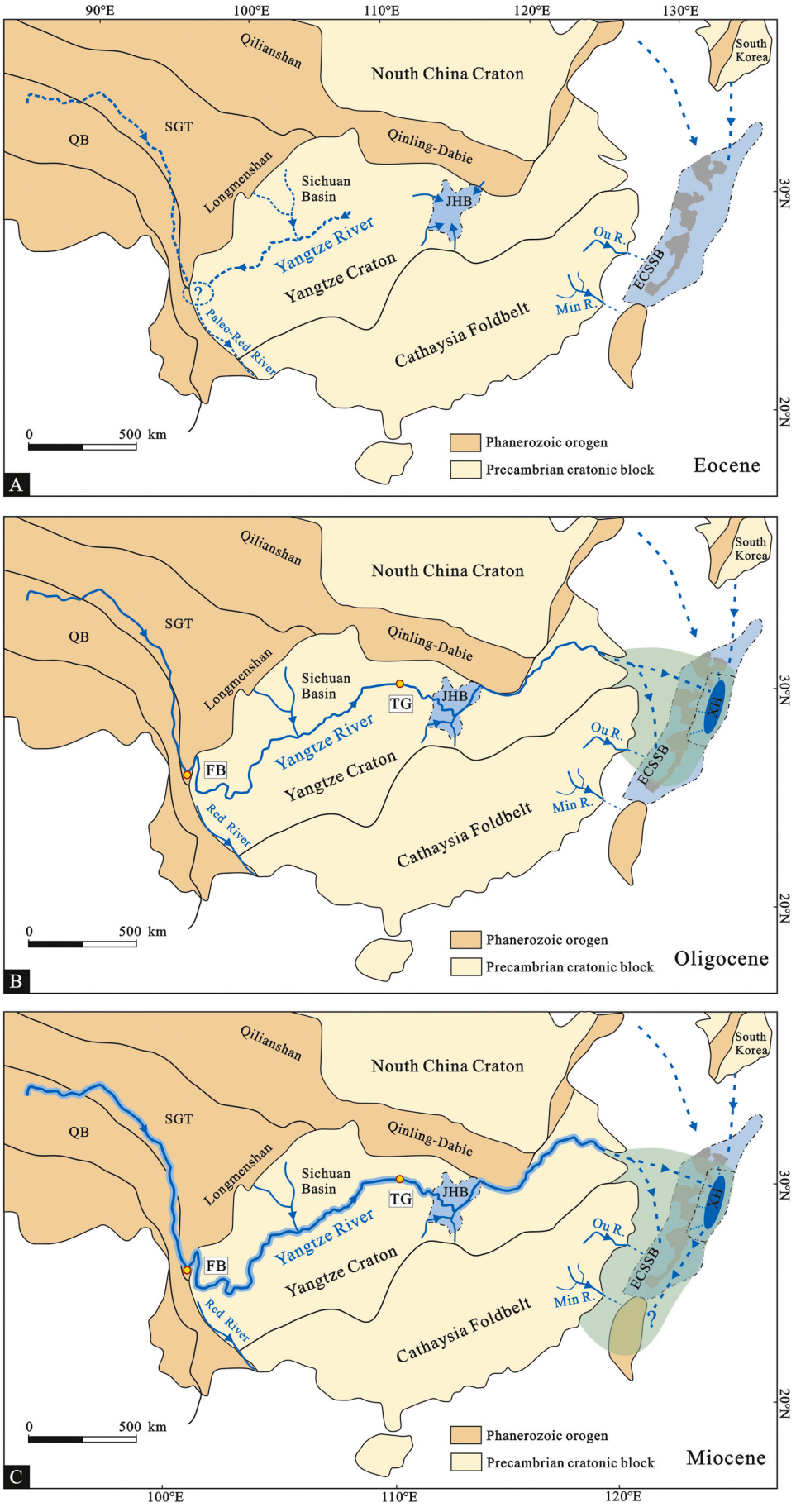

Fig. 5. Schematic maps showing the development of the Yangtze River (modified from Zheng et al., 2013a; Zhang et al., 2017; Wang et al., 2018), based on the tectonic framework of China (Zheng et al., 2013b; Zheng, 2015). A) Eocene; B) Oligocene; C) Miocene. ECSSB: East China Sea Shelf Basin; XH: Xihu Depression; JHB: Jianghan Basin; TG: Three Gorge; SB: Sichuan Basin; FB: First Bend; QB: Qingtang Block; SGT: Songpan-Garze Terrane. The green shade denotes the area of Yangtze River drainage. (For interpretation of the references to colour in this figure legend, the reader is referred to the web version of this article.)

of earlier rift-related structures is well-documented on the East China shelf, which may provide favorable conditions for sediment recirculation and transport. The inversion began in the Oligocene and was centered predominantly on the eastern part of the ECSSB, along the Diaoyu Islands Folded-Uplift Belt (Taiwan-Sinzi belt) (Wang et al., 2018). In the Miocene, compression and inversion migrated to the Xihu Depression, and formed a series of NE-trending anticlines in the areas of former subsidence and sedimentation (Zhou et al., 2001; Guo et al., 2015; Zhang et al., 2016). The ECSSB has the characteristics of a southward tilted terrain (Zhang et al., 2017) and the main sediment transport directions in the Oligocene deposits are directed southwards (Zhang et al., 2018). The structural highs in the Diaoyu Islands Folded-Uplift Belt to the east of the basin prevent eastward transport of sediment (Wang et al., 2018). Therefore, most of sediments delivered by the Yangtze River are thought to have drained southward and a sediment transport pathway may be formed between the ECSSB and proto-Taiwan.

The depositional environment in the ECSSB has changed from tidal-deltaic deposits of the lower Oligocene Pinghu Formation to dominated fluvial deposits of the lower Miocene Longjing Formation, revealing the retreat of coastlines and the expansion of the drainage area. The Oligocene-Miocene strata in the offshore basins north of Taiwan are interpreted as fluvial to coastal deposits (Chou, 1970; Yu and Chow, 1997; Huang et al., 2012), in agreement with an increased southward sediment transport (Zhang et al., 2017). Our Monte Carlo model results also indicate an increase in transport capacity and coverage of the Yangtze River drainage. Therefore, we consider it likely that the Oligocene Yangtze drainage area was restricted to the northern basins (e.g., Xihu Depression) of the ECSSB, and that this drainage area in the Miocene, under a stable supply of sediment sources, extended southwards to the Taiwanese margin (Fig. 5).

5.3. Paleogeographic and paleoclimatic constraints

The two river capture points along the Yangtze River provide further constraints on the initiation of its modern flow system: the First Bend and the Three Gorges (Xiang et al., 2007) (FB and TG in Fig. 5). A connection between the Yangtze drainage and the ECSSB implies that the First Bend was formed and the Three Gorges was channelized. The formation of the First Bend was recently dated to the late Eocene, based on U—Pb dating of detrital zircons from the Jianchuan Basin and its adjacent region (Fig. 5A; Zheng et al., 2020). Surface uplift and inversion of the Jianchuan Basin, established at ca. 35 Ma, caused the paleo-Yangtze, until that time flowing southwards to the South China Sea, to be diverted towards the northeast in the direction of the modern Yangtze system, draining into the ECSSB. The formation time of the Three Gorges post-dates the late Eocene, based on the termination of evaporite deposition in the Jianghan Basin, downstream of the Three Gorges (Fig. 5B; Zheng et al., 2013a). Consequently, evaporite sedimentation must have precluded major river flow and that the Yangtze River was thus initiated after Jianghan evaporite formation, dated to the late Eocene (ca. 36.5 Ma). In addition, it was concluded that the Three Gorges must have originated before 23 Ma, based on $^{40}Ar/^{39}Ar$ ages and detrital zircon U—Pb ages from basalts and riverine sediments from the lower reaches of the Yangtze (Zheng et al., 2013a). These results are thus in good agreement with the presence of Yangtze River drainage in the Oligocene deposits of the ECSSB,

Seasonal storms of the South and East Asian monsoons cause the majority of precipitation to continental interiors of India and China, hence regulating runoff (Clift et al., 2008a), which implies that sediment flux to the oceans surrounding Asia is mostly related to monsoon intensity. High precipitation rates generally boost river transport capacity and promote soil erosion across the river basin (Zong et al., 2010), resulting in coarser-grained sediment being accessible for river transport (Nan et al., 2014). Sediment flow from Asia generally increased in the Oligocene (< 33 Ma) and peaked in the early–middle Miocene (24–11 Ma), far before the onset of a glacial climate. This demonstrates that in east Asia rock uplift and particular precipitation are the primary constraints on erosion, at least over long geologic time scales (Clift, 2006, 2010). The Miocene East Asian monsoon strengthening (e.g., Sun and Wang, 2005; Clift et al., 2008a; Guo et al., 2008), combined with the intensification of river flow, transport capacity, and erosion of the Three Gorges in the Yangtze River, all indicate that the east Asian rivers could probably carry more sediments and move further south (e.g., Zhang et al., 2017) (Fig. 5C). Under the Asian monsoon evolution setting, this continental-scale river should have been a perennial stream during the early to middle-Miocene (Zheng et al., 2013a). The increase in the contribution of the Yangtze River accordingly explains the increase in the proportions of ~790 Ma component in Miocene sediments (Table S1) and the Monte Carlo model results (Fig. 4B). We furthermore envisage that in the Oligocene a topographic barrier prevented the Yangtze River drainage to cover the southwestern ECSSB and Taiwan areas, but detailed information on basin evolution and transport pathways are still lacking.

6. Conclusions

The analysis of detrital zircon U—Pb ages of the Pinghu, Huagang, and Longjing formations in the Xihu Depression of ECSSB indicates similar age distributions as observed in modern Yangtze River sediments. We therefore conclude that the Yangtze River is one of the main sediment sources in the Xihu Depression since at least the early Oligocene (Fig. 5). However, the supply of additional sources (e.g., South Korean rivers, North China Craton rivers, and neighbouring margins) is necessary to explain the relatively low proportion of ~790 Ma components in the KDEs of the ECSSB. This implies that the modern Yangtze River was initiated before the Oligocene with a major drainage system towards the ECSSB. In agreement with recent chronological updates on the Pinghu Formation, the First Bend, and the Three Gorges, we conclude that a modern-type Yangtze drainage was established at an age of ca. 34 Ma. In the Miocene (< 23 Ma), the Yangtze drainage system extended further southwards to the southwestern ECSSB and the marginal basins of modern Taiwan, possibly related to stronger monsoons, increased sediment transport, and a southward tilting of the ECSSB.

Supplementary data to this article can be found online at https://doi.org/10.1016/j.palaeo.2021.110548.

Declaration of Competing Interest

The authors declare that they have no known competing financial interests or personal relationships that could have appeared to influence the work reported in this paper.

Acknowledgments

This research was funded by the National Natural Science Foundation of China (No. 41690131), National Science and Technology Major Project of China (2016ZX05027-001 and 2017ZX05049-004), China Scholarship Council (CSC), and Fundamental Research Funds for National Universities, China University of Geosciences, Wuhan. We thank CNOOC Shanghai Branch for providing access to their geological data and boreholes. We thank Licheng Cao for beneficial discussions on the statistical analysis. We thank editor Paul Hesse, and two anonymous reviewers for their thorough and constructive comments that significantly improved the manuscript.

References

Abbas, A., Zhu, H., Zeng, Z., Zhou, X., 2018. Sedimentary facies analysis using sequence stratigraphy and seismic sedimentology in the Paleogene Pinghu Formation, Xihu Depression, East China Sea Shelf Basin. Mar. Pet. Geol. 93, 287–297.

Cao, L., Shao, L., Qiao, P., Cui, Y., Zhang, G., Zhang, X., 2020. Formation and paleogeographic evolution of the Palawan continental terrane along the Southeast Asian margin revealed by detrital fingerprints. GSA Bull. 133, 1167–1193.
Chou, J., 1970. A stratigraphic and sedimentary analysis of the miocene in Northern Taiwan. Petrol. Geol. Taiwan 7, 145–189.
Chough, S., Kwon, S.-T., Ree, J.-H., Choi, D., 2000. Tectonic and sedimentary evolution of the Korean peninsula: a review and new view. Earth-Sci. Rev. 52, 175–235.
Clark, M., Schoenbohm, L., Royden, L., Whipple, K., Burchfiel, B., Zhang, X., Tang, W., Wang, E., Chen, L., 2004. Surface uplift, tectonics, and erosion of eastern Tibet from large-scale drainage patterns. Tectonics 23, TC1006.
Clift, P.D., 2006. Controls on the erosion of Cenozoic Asia and the flux of clastic sediment to the ocean. Earth Planet. Sci. Lett. 241, 571–580.
Clift, P.D., 2010. Enhanced global continental erosion and exhumation driven by Oligo-Miocene climate change. Geophys. Res. Lett. 37, L09402.
Clift, P.D., Hodges, K.V., Heslop, D., Hannigan, R., Van Long, H., Calves, G., 2008a. Correlation of Himalayan exhumation rates and Asian monsoon intensity. Nat. Geosci. 1, 875–880.
Clift, P.D., Long, H.V., Hinton, R., Ellam, R.M., Hannigan, R., Tan, M.T., Blusztajn, J., Duc, N.A., 2008b. Evolving east Asian river systems reconstructed by trace element and Pb and Nd isotope variations in modern and ancient Red River-Song Hong sediments. Geochem. Geophys. Geosyst. 9, Q04039.
Compston, W., Williams, I., Kirschvink, J., Zichao, Z., Guogan, M., 1992. Zircon U-Pb ages for the Early Cambrian time-scale. J. Geol. Soc. 149, 171–184.
Ding, R., Zou, H., Min, K., Yin, F., Du, X., Ma, X., Su, Z., Shen, W., 2017. Detrital zircon U-Pb geochronology of Sinian-Cambrian strata in the Eastern Guangxi area, China. J. Earth Sci. 28, 295–304.
Feng, L., Lu, Y.C., Wellner, J.S., Liu, J.S., Liu, X.F., Li, X.Q., Zhang, J.Y., 2019. Fluvial morphology and reservoir sand-body architecture in lacustrine rift basins with axial and lateral sediment supplies: oligocene fluvial–lacustrine succession in the Xihu sag, East China Sea Shelf Basin. Aust. J. Earth Sci. 67, 279–304.
Fu, X., Zhu, W., Geng, J., Yang, S., Zhong, K., Huang, X., Zhang, L., Xu, X., 2020. The present-day Yangtze River was established in the late Miocene: evidence from detrital zircon ages. J. Asian Earth Sci. 104600.
Guo, Z., Sun, B., Zhang, Z., Peng, S., Xiao, G., Ge, J., Hao, Q., Qiao, Y., Liang, M., Liu, J., 2008. A major reorganization of Asian climate by the early Miocene. Clim. Past 4, 153–174.
Guo, Z., Liu, C., Tian, J., 2015. Structural characteristics and main controlling factors of inversion structures in Xihu Depression in Donghai Basin. Earth Sci. Front. 22, 59–67 (in Chinese with English Abstract).
Hao, L., Wang, Q., Guo, R., Tuo, C., Ma, D., Mou, W., Tian, B., 2018a. Diagenetic fluids evolution of Oligocene Huagang Formation sandstone reservoir in the south of Xihu Sag, the East China Sea Shelf Basin: constraints from petrology, mineralogy, and isotope geochemistry. Acta Oceanol. Sin. 37, 25–34 (in Chinese with English abstract).
Hao, L., Wang, Q., Tao, H., Li, X., Ma, D., Ji, H., 2018b. Geochemistry of Oligocene Huagang formation clastic rocks, Xihu sag, the East China Sea Shelf Basin: provenance, source weathering, and tectonic setting. Geol. J. 53, 397–411.
He, M., Zheng, H., Clift, P.D., 2013. Zircon U–Pb geochronology and Hf isotope data from the Yangtze River sands: Implications for major magmatic events and crustal evolution in Central China. Chem. Geol. 360-361, 186–203.
He, M., Zheng, H., Bookhagen, B., Clift, P.D., 2014. Controls on erosion intensity in the Yangtze River basin tracked by U–Pb detrital zircon dating. Earth-Sci. Rev. 136, 121–140.
Huang, J., Ren, J., Jiang, C., 1977. The basic outline of China tectonics. Acta Geol. Sin. 52, 117–135 (in Chinese with English abstract).
Huang, C.-Y., Yen, Y., Zhao, Q., Lin, C.-T., 2012. Cenozoic stratigraphy of Taiwan: Window into rifting, stratigraphy and paleoceanography of South China Sea. Chin. Sci. Bull. 57, 3130–3149.
Lan, Q., Yan, Y., Huang, C.-Y., Santosh, M., Shan, Y.-H., Chen, W., Yu, M., Qian, K., 2016. Topographic architecture and drainage reorganization in Southeast China: zircon U-Pb chronology and Hf isotope evidence from Taiwan. Gondwana Res. 36, 376–389.
Lee, H., Jeong, K., Han, S., Bahk, K., 1988. Heavy minerals indicative of Holocene transgression in the southeastern Yellow Sea. Cont. Shelf Res. 8, 255–266.
Li, J., Xie, S., Kuang, M., 2001. Geomorphic evolution of the Yangtze Gorges and the time of their formation. Geomorphology 41, 125–135.
Li, S., Yu, X., Steel, R., Zhu, X., Li, S., Cao, B., Hou, G., 2018. Change from tide-influenced deltas in a regression-dominated set of sequences to tide-dominated estuaries in a transgression-dominated sequence set, East China Sea Shelf Basin. Sedimentology 65, 2312–2338.
Liang, R., Zheng, Y., Wang, K., 2006. Study on magnetic anomalies in the hupijiao reef and adjacent sea areas in the Northern East China Sea. Adv. Mar. Sci. 24, 173 (in Chinese with English Abstract).
Liu, Y., Hu, Z., Gao, S., Günther, D., Xu, J., Gao, C., Chen, H., 2008. In situ analysis of major and trace elements of anhydrous minerals by LA-ICP-MS without applying an internal standard. Chem. Geol. 257, 34–43.
Métivier, F., Gaudemer, Y., Tapponnier, P., Klein, M., 1999. Mass accumulation rates in Asia during the Cenozoic. Geophys. J. Int. 137, 280–318.
Milliman, J.D., Farnsworth, K.L., 2013. River Discharge to the Coastal Ocean: A Global Synthesis. Cambridge University Press, New York.
Nan, Q., Li, T., Chen, J., Nigma, R., Yu, X., Xu, Z., Yang, Z., 2014. Late Holocene (~2 ka) East Asian Monsoon variations inferred from river discharge and climate interrelationships in the Pearl River Estuary. Quat. Res. 81, 240–250.
Ren, J., Tamaki, K., Li, S., Junxia, Z., 2002. Late Mesozoic and Cenozoic rifting and its dynamic setting in Eastern China and adjacent areas. Tectonophysics 344, 175–205.
Richardson, N.J., Densmore, A.L., Seward, D., Wipf, M., Yong, L., 2010. Did incision of the Three Gorges begin in the Eocene? Geology 38, 551–554.
Saylor, J.E., Jordan, J.C., Sundell, K.E., Wang, X., Wang, S., Deng, T., 2018. Topographic growth of the Jishi Shan and its impact on basin and hydrology evolution, NE Tibetan Plateau. Basin Res. 30, 544–563.
Shao, L., Cao, L., Pang, X., Jiang, T., Qiao, P., Zhao, M., 2016. Detrital zircon provenance of the Paleogene syn-rift sediments in the northern South China Sea. Geochem. Geophys. Geosyst. 17, 255–269.
Sun, X., Wang, P., 2005. How old is the Asian monsoon system?-Palaeobotanical records from China. Palaeogeogr. Palaeoclimatol. Palaeoecol. 222, 181–222.
Su, A., Chen, H., Zhao, J., Zhang, T., Feng, Y., Wang, C., 2020. Natural gas washing induces condensate formation from coal measures in the Pinghu Slope Belt of the Xihu Depression, east China Sea basin: Insights from fluid inclusion, geochemistry, and rock gold-tube pyrolysis. Mar. Pet. Geol., 104450 https://doi.org/10.1016/j.marpetgeo.2020.104450.
Sun, X., Kuiper, K.F., Wang, J., Tian, Y., Vermeesch, P., Zhang, Z., Zhao, J., Wijbrans, J. R., 2018. Geochronology of detrital muscovite and zircon constrains the sediment provenance changes in the Yangtze River during the late Cenozoic. Basin Res. 30, 636–649.
Sundell, K.E., Saylor, J.E., 2017. Unmixing detrital geochronology age distributions. Geochem. Geophys. Geosyst. 18, 2872–2886.
Suo, Y., Li, S., Zhao, S., Somerville, I., Yu, S., Dai, L., Xu, L., Cao, X., Wang, P., 2015. Continental margin basins in East Asia: tectonic implications of the Meso-Cenozoic East China Sea pull-apart basins. Geol. J. 50, 139–156.
Van Hoang, L., Wu, F.Y., Clift, P.D., Wysocka, A., Swierczewska, A., 2009. Evaluating the evolution of the Red River system based on in situ U-Pb dating and Hf isotope analysis of zircons. Geochem. Geophys. Geosyst. 10.
Vermeesch, P., 2013. Multi-sample comparison of detrital age distributions. Chem. Geol. 341, 140–146.
Wang, P., 2004. Cenozoic deformation and the history of sea-land interactions in Asia. Geophys. Monogr. Ser. 149, 1–22.
Wang, J., Yang, Y., Shao, L., 2010. Detrital zircon geochronology and provenance of core sediments in Zhoulao Town, Jianghan plain, China. J. Earth Sci. 21, 257–271.
Wang, W., Bidgoli, T., Yang, X., Ye, J., 2018. Source-to-sink links between East Asia and Taiwan from detrital zircon geochronology of the Oligocene Huagang Formation in the East China Sea Shelf Basin. Geochem. Geophys. Geosyst. 19, 3673–3688.
Weislogel, A., Graham, S., Chang, E., Wooden, J., Gehrels, G., 2010. Detrital zircon provenance from three turbidite depocenters of the Middle–Upper Triassic Songpan-Ganzi complex, central China: record of collisional tectonics, erosional exhumation, and sediment production. GSA Bull. 122, 2041–2062.
Wiedenbeck, M., Alle, P., Corfu, F., Griffin, W., Meier, M., Oberli, F.v., Quadt, A.v., Roddick, J., Spiegel, W., 1995. Three natural zircon standards for U-Th-Pb, Lu-Hf, trace element and REE analyses. Geostand. Newslett. 19, 1–23.
Wu, J., 2016. Discovery of Tidal Sand Ridges and its significance of Pinghu formation in Xihu depression. Acta Sedimentol. Sin. 34, 924–929 (in Chinese with English abstract).
Xia, Y., Xu, X.-S., Zhu, K.-Y., 2012. Paleoproterozoic S-and A-type granites in southwestern Zhejiang: magmatism, metamorphism and implications for the crustal evolution of the Cathaysia basement. Precambrian Res. 216, 177–207.
Xiang, F., Zhu, L., Wang, C., Zhao, X., Chen, H., Yang, W., 2007. Quaternary sediment in the Yichang area: implications for the formation of the Three Gorges of the Yangtze River. Geomorphology 85, 249–258.
Xu, Y., 2017. Comment on "Detrital zircon geochronology of river sands from Taiwan: Implications for sedimentary provenance of Taiwan and its source link with the east China mainland" by Deng K, Yang SY, Li C, Su N, Bi L, Chang YP, Chang SC.[Earth-Science Reviews 164 (2017), 31–47]. Earth-Sci. Rev. 168, 232–234.
Yan, Y., Carter, A., Palk, C., Brichau, S., Hu, X., 2011. Understanding sedimentation in the Song Hong–Yinggehai Basin, South China Sea. Geochem. Geophys. Geosyst. 12, Q06014.
Yang, X., Li, A., Qin, Y., Wu, S., Wu, Z., Zhang, J., 2006. U-Pb dating of zircons from cenozoic sandstone: constrain on the geodynamic setting of East China Sea Shelf Basin. Mar. Geol. Quat. Geol. 26, 75–86.
Yang, W.D., Cui, Z.K., Zhang, Y.B., 2010. Geology and Mineral Resources of East China Sea. Ocean Press, Beijing (in Chinese).
Yang, C., Shen, C., Zattin, M., Yu, W., Shi, S., Mei, L., 2019. Provenances of Cenozoic sediments in the Jianghan Basin and implications for the formation of the Three Gorges. Int. Geol. Rev. 61, 1980–1999.
Ye, J., Qing, H., Bend, S.L., Gu, H., 2007. Petroleum systems in the offshore Xihu Basin on the continental shelf of the East China Sea. AAPG Bull. 91, 1167–1188.
Yu, H.-S., Chow, J., 1997. Cenozoic basins in northern Taiwan and tectonic implications for the development of the eastern Asian continental margin. Palaeogeogr. Palaeoclimatol. Palaeoecol. 131, 133–144.
Yu, J.-H., O'Reilly, S.Y., Wang, L., Griffin, W.L., Zhou, M.-F., Zhang, M., Shu, L., 2010. Components and episodic growth of Precambrian crust in the Cathaysia Block, South China: evidence from U–Pb ages and Hf isotopes of zircons in Neoproterozoic sediments. Precambr. Res. 181, 97–114.
Yue, W., Liu, J.T., Zhang, D., Wang, Z., Zhao, B., Chen, Z., Chen, J., 2016. Magnetite with anomalously high Cr2O3 as a fingerprint to trace upper Yangtze sediments to the sea. Geomorphology 268, 14–20.
Zhai, M.-G., Santosh, M., 2011. The early Precambrian odyssey of the North China Craton: a synoptic overview. Gondwana Res. 20, 6–25.
Zhai, M., Guo, J., Liu, W., 2005. Neoarchean to Paleoproterozoic continental evolution and tectonic history of the North China Craton: a review. J. Asian Earth Sci. 24, 547–561.
Zhang, J., Xu, F., Zhong, T., Zhang, T., Yu, Y., 2012. Sequence stratigraphic models and sedimentary evolution of Pinghu and Huagang formations in xihu trough. Mar. Geol. Quat. Geol. 32, 35–42 (in Chinese with English Abstract).

Zhang, G., Li, S., Suo, Y., Zhang, J., 2016. Cenozoic positive inversion tectonics and its migration in the East China Sea Shelf Basin. Geol. J. 51, 176–187.
Zhang, X., Huang, C., Wang, Y., Clift, P.D., Yan, Y., Fu, X., Chen, D., 2017. Evolving Yangtze River reconstructed by detrital zircon U-Pb dating and petrographic analysis of Miocene marginal Sea sedimentary rocks of the Western Foothills and Hengchun Peninsula, Taiwan. Tectonics 36, 634–651.
Zhang, J., Lu, Y., Krijgsman, W., Liu, J., Li, X., Du, X., Wang, C., Liu, X., Feng, L., Wei, W., Lin, H., 2018. Source to sink transport in the Oligocene Huagang Formation of the Xihu Depression, East China Sea Shelf Basin. Mar. Pet. Geol. 98, 733–745.
Zhang, J., Pas, D., Krijgsman, W., Wei, W., Du, X., Zhang, C., Liu, J., Lu, Y., 2020. Astronomical forcing of the Paleogene coal-bearing hydrocarbon source rocks of the East China Sea Shelf Basin. Sediment. Geol. 406, 105715.
Zhao, G., Cawood, P.A., 2012. Precambrian geology of China. Precambrian Res. 222, 13–54.
Zhao, Z., Zhai, M., Wang, K., Yan, Y., Guo, J., Liu, Y., 1993. Precambrian Crustal Evolution of the Sino-Korean Paraplatform. Science Press, Beijing, pp. 366–384 (in Chinese).
Zhao, G., Sun, M., Wilde, S.A., Sanzhong, L., 2005. Late Archean to Paleoproterozoic evolution of the North China Craton: key issues revisited. Precambrian Res. 136, 177–202.
Zhao, L., Chen, J., Zhang, Y., 2008. Sedimentary characteristics of Pinghu Formation in Pinghu structural belt of Xihu Depression, East China Sea. Glob. Geol. 27, 42–47 (in Chinese with English abstract).
Zheng, H., 2015. Birth of the Yangtze River: age and tectonic-geomorphic implications. Natl. Sci. Rev. 2, 438–453.
Zheng, J., Griffin, W., O'Reilly, S.Y., Zhang, M., Pearson, N., Pan, Y., 2006. Widespread Archean basement beneath the Yangtze craton. Geology 34, 417–420.
Zheng, H., Clift, P.D., Wang, P., Tada, R., Jia, J., He, M., Jourdan, F., 2013a. Pre-Miocene birth of the Yangtze River. Proc. Natl. Acad. Sci. U. S. A. 110, 7556–7561.
Zheng, Y., Xiao, W., Zhao, G., 2013b. Introduction to tectonics of China. Gondwana Res. 23, 1189–1206.
Zheng, H., Clift, P.D., He, M., Bian, Z., Liu, G., Liu, X., Xia, L., Yang, Q., Jourdan, F., 2020. Formation of the first Bend in the late Eocene gave birth to the modern Yangtze River, China. Geology. https://doi.org/10.1130/G48149.1.
Zhou, Z., Jiang, J., Liao, Z., Yang, F., Shang, K., 2001. Basin inversion in Xihu Depression, East China Sea. Gondwana Res. 4, 844–845.
Zhu, W., Mi, L., Zhang, H., 2010. Atlas of Oil and Gas Basins, China Sea. Petroleum Industry Press, Beijing, pp. 73–75 (in Chinese).
Zhu, Y., Li, Y., Zhou, J., Gu, S., 2012. Geochemical characteristics of Tertiary coal-bearing source rocks in Xihu Depression, East China Sea Basin. Mar. Pet. Geol. 35, 154–165.
Zong, Y., Yu, F., Huang, G., Lloyd, J.M., Yim, W.S., 2010. Sedimentary evidence of late Holocene human activity in the Pearl River delta, China. Earth Surf. Process. Landforms 35, 1095–1102.